

# Tomography for Local Plasma Turbulence Measurements

Akihide FUJISAWA, Yoshihiko NAGASHIMA and Shigeru INAGAKI

Research Institute for Applied Mechanics and Research Center for Plasma Turbulence, Kyushu University,  
Kasuga Kohen, Kasuga, Fukuoka 816-8580, Japan

(Received 8 August 2015 / Accepted 25 August 2015)

A prototype system for plasma turbulence tomography was tested in linear plasma with aiming at future application to toroidal plasma. The line-integrated plasma emission lines of ArI and ArII were measured with sufficiently high signal-to-noise ratios, and the signals were reconstructed using the maximum likelihood expectation maximization (MLEM) algorithm and parallel computing. Here, the first results for local plasma emissions and fluctuation spectra obtained with the prototype system are reported.

© 2015 The Japan Society of Plasma Science and Nuclear Fusion Research

Keywords: plasma turbulence, turbulence tomography, MLEM, local emission fluctuation

DOI: 10.1585/pfr.10.1201080

Plasma turbulence is ubiquitous in the laboratory, nature and the universe. At present, plasma turbulence has been recognized as a system of microscale drift waves with meso and macrostructures, such as zonal flows and streamers [1–3]. These elemental components are interacting with each other to form the turbulent plasma structure and dynamics. Progress in understanding of plasma turbulence requires new innovative diagnostic methods that can measure the plasma turbulence structures in the entire plasma region from micro- to macroscales.

Computed tomography (CT) satisfies such requirements, and can measure the entire plasma region, in a sufficiently wide range of spatiotemporal scales. A prototype system has been built and installed on the linear cylindrical plasma, plasma assembly for nonlinear turbulence analysis (PANTA) [4]. Trial experiments have been performed using argon plasma discharges. In this study, we describe the development of the diagnostic system, and present the first results successfully obtained with this system, *i.e.* local plasma emission distribution and its local emission fluctuations.

The PANTA linear cylindrical device produces helicon plasmas of 5 cm radius with discharge duration of approximately 0.6 s in a 0.09 T straight magnetic field. Figure 1 shows a schematic view of the tomography system, with which we observe the line-integrated plasma emissions from four azimuthal directions at 45 degree to each other. Each light guide array contains 33 fiber channels, and consists of collimators, optical filters, and optical feedthrough that transfers the optically filtered light to the atmosphere side. The collimators (or fiber channels) are aligned by every 5 mm in the range from  $L = -8$  to  $L = 8$  cm. The plasma light is passed through optical fibers to the photodiode detectors with gain and frequency bandwidth of  $10^8$  V/A and up to 50 kHz, respec-

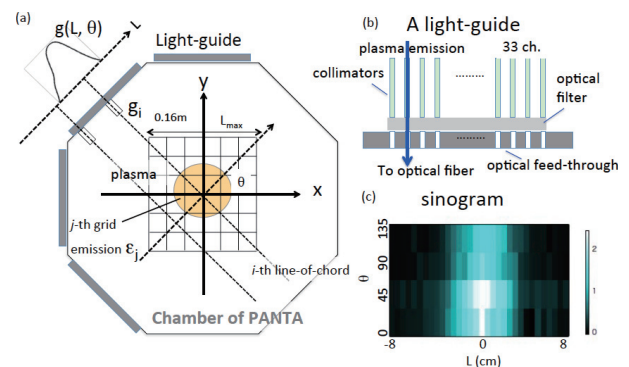


Fig. 1 (a) Geometry of the tomography system and corresponding definition of coordinates. (b) Schematic view of the light guide. (c) Sinogram of ArI.

tively. The noise of the detection system depends on the amplifier noise level, which is less than  $\pm 50$  mV. Plasma emission was observed with two wavelength bands around the strong lines of ArI (810 nm) and ArII (476.5 nm) lines for the discharges of low-filling pressure of  $\sim 2$  mT. The ArI and ArII emissions are measured at the plasma cross section at a distance of 62.5 cm and 37.5 cm, respectively, from the plasma-producing antenna. Line-integrated data are plotted on  $\theta$  and  $L$  axes and shown as sinograms. Figure 1 (c) shows the sinogram of the temporally averaged ArI emission in a steady state from 0.2 s to 0.4 s.

To deduce local emissions, the series expansion methods [5, 6] may regulate the reconstructed images using assumed function forms but can not account for spatially discrete changes that are expected in plasma with strong non-linearity. Therefore, the maximum likelihood expectation maximization (MLEM) algorithm [7] without any a priori assumptions, which has been developed for medical applications, was selected for the tomography reconstruction. The reconstructed tomography images using MLEM are

author's e-mail: fujisawa@triam.kyushu-u.ac.jp

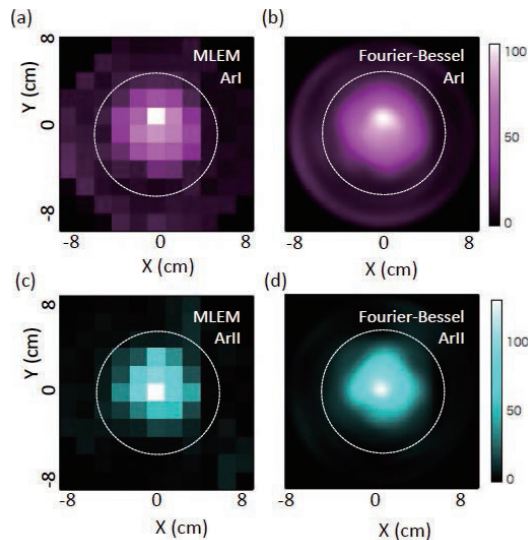


Fig. 2 (a) Reconstructed local emission of ArI with MLEM, and (b) the corresponding image obtained with the fitting of Fourier–Bessel series expansion. (c) Reconstructed local emission of ArII with MLEM, and (d) the corresponding image obtained with the fitting of Fourier–Bessel series expansion. The dashed circles represent the shape of the antenna that generates the plasma.

shown in Fig. 2. The obtained local values are calculated on  $121 (= 11 \times 11)$  grids on a  $16 \text{ cm} \times 16 \text{ cm}$  observation square with grid width of  $\sim 1.5 \text{ cm}$ . Increasing the number of the channels is essential to obtain *continuous* images with finer spatial resolution. Figure 2 also shows the mosaic image obtained with MLEM and the fitting image obtained with the Fourier–Bessel function series.

The experimental sinograms for the whole discharge can be converted into the reconstructed images for each sampling time, in this case  $1 \mu\text{s}$ . The tomography data for a single shot are huge about  $0.32 \text{ GB}$  for a shot. To manage such a huge amount of data, the tomographic reconstruction is performed using parallel processing on 10 Power macintosh computers with totally 12-core CPUs ( $2 \times 2.4 \text{ GHz}$  6-Core Intel Xeon).

The local waveforms of the ArI and ArII emissions are obtained as the 121 grid values on the observation square using MLEM and parallel computing. Figure 3 shows the local waveforms of the ArI emission at  $(x, y) = (-1.5, -1.5) \text{ cm}$  and the ArII emission at the center of the observation square,  $(x, y) = (0, 0) \text{ cm}$ . The corresponding wavelet and fast Fourier transform (FFT) spectra are also shown in Fig. 3. The wavelet spectra demonstrate the intermittent nature of the emission fluctuations [8], whereas the FFT spectra calculated as averages from  $0.2 \text{ s}$  to  $0.4 \text{ s}$  show the presence of coherent activities in the fluctuations. The noise levels owing to the amplifier noise are also shown in the plots of FFT spectra. This shows that the local emissions and their power spectra can be successfully obtained for good signal-to-noise ratio.

In summary, the proposed turbulence diagnostic

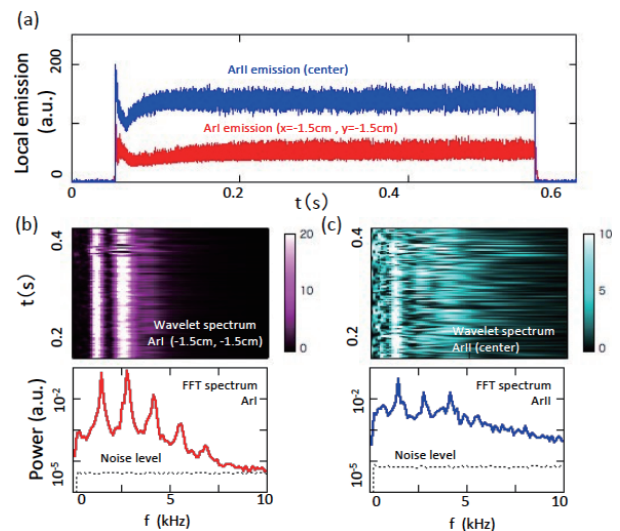


Fig. 3 (a) Local emission waveforms of ArI and ArII. (b) The corresponding wavelet and FFT spectra of ArI at a position of  $\sim 2 \text{ cm}$  away from the center of the observation square, and (c) wavelet and FFT spectra of ArII emission at the center. The scale of the wavelet spectra is linear.

method appears promising. Moreover, PANTA is non-perturbative, and it is hence possible to access the plasma core region where drastic changes in plasma properties inhibit the insertion of traditional probes. The proposed tomography method can address the missing link between central core and periphery in dynamic phenomena [9, 10]. Finally, the ultimate goal of this study is to apply an extended system on magnetically confined high-temperature plasmas. This requires a magnetically confined torus plasma specially designed for turbulence tomography.

## Acknowledgments

This work was partly supported by the Grant-in-Aids for Scientific Research (Nos. 21224014, 23246162, 26420852, and 15H02335).

- [1] P.H. Diamond, S.-I. Itoh, K. Itoh and T.S. Hahm, *Plasma Phys. Control. Fusion* **47**, R35 (2005).
- [2] A. Fujisawa, *Nucl. Fusion* **49**, 013001 (2009).
- [3] G.R. Tynan, A. Fujisawa and G. McKee, *Plasma Phys. Control. Fusion* **51**, 113001 (2009).
- [4] S. Oldenbürger, S. Inagaki, T. Kobayashi *et al.*, *Plasma Phys. Control. Fusion* **54**, 055002 (2012).
- [5] A.M. Cormack, *J. Appl. Phys.* **35**, 2908 (1964).
- [6] Y. Nagayama, *J. Appl. Phys.* **62**, 2702 (1987).
- [7] L.A. Shepp and Y. Vardi, *IEEE Trans. Med. Imag.* **1**, 113 (1982).
- [8] B. Ph. van Milligen, C. Hidalgo and E. Sánchez, *Phys. Rev. Lett.* **74**, 395 (1995).
- [9] T. Yamada, S.-I. Itoh, T. Maruta *et al.*, *Nature Phys.* **4**, 721 (01 Sep. 2008).
- [10] H. Arakawa, T. Kobayashi, S. Inagaki *et al.*, *Plasma Phys. Control. Fusion* **53**, 115009 (2011).